

Maxwell's equal-area law for Vaidya-Bonner-de Sitter black hole under Lorentz invariance violation

Yenshembam Priyobarta Singh¹ ‡, Telem Ibungochouba Singh^{1,*} §, Sapam Niranjana Singh¹ ||

¹ Department of Mathematics, Manipur University, Canchipur, Imphal 795003, Manipur, India

Abstract. In this paper, we investigate the tunneling of fermions with arbitrary spin near the event horizon of non-stationary Vaidya-Bonner-de Sitter black hole (VBdS) in Lorentz invariance violation (LIV). The modified Hawking temperature of VBdS black holes is calculated by using tortoise coordinate transformation, Feynman prescription and WKB approximation. By considering cosmological constant as a thermodynamic pressure in the extended phase space, we construct Maxwell's equal-area law in LIV and study the phase transitions of VBdS black hole in $P - \tilde{v}$, $P - V$ and $T - S$ plane. The LIV increases the length of liquid-gas coexistence region. The thermodynamic quantities such as entropy, heat capacity, Helmholtz free energy, Internal energy, enthalpy and Gibbs free energy of VBdS black hole are discussed. These quantities tend to increase under LIV. The stability of black hole is also discussed in the presence of LIV.

Keywords: Hawking temperature, Lorentz invariance violation, Maxwell's equal-area law, Entropy

‡ E-mail: priyoyensh@gmail.com

§ * E-mail: ibungochouba@rediffmail.com

|| E-mail: sapamkhomba@gmail.com

1. Introduction

The LIGO and Virgo observations, as well as the M87* black hole shadow captured by Event Horizon Telescope, have proven the existence of black holes [1–5]. Since then, the study of black holes and their properties become more relevant and fascinating subjects among the researchers. The Hawking temperature is a key concept in black hole thermodynamics and it has a great significance in understanding the nature of black holes. Hawking [6, 7] proposed the thermal radiation for studying the quantum effects near the event horizon of black hole. Several methods for calculating the Hawking temperature of black holes are found in the literatures [8–11]. The semiclassical tunneling method proposed by Kraus, Parikh and Wilczek [12–15] for deriving Hawking temperature is widely used to study the Hawking temperature for different types of black holes. In these papers, the radial null geodesic method is used to derive the Hawking temperature in accordance with the semi-classical WKB approximation. Another tunneling method to derive Hawking temperature is the Hamilton-Jacobi method [16] which is an extension of the complex path analysis of Padmanabhan et al. work [17–19]. Many remarkable results were obtained using this technique in [20–25]. Ref. [26, 27] corrected the tunneling probability after considering the effects of backreaction and self-gravitation to study the Hawking temperature and semi-classical black hole entropy. The effects of the GUP in the tunneling formalism for Hawking radiation is widely studied in [28–37] and calculated the quantum corrected Hawking temperature.

According to the study of string theory and quantum gravity theory, Lorentz invariance, which is a fundamental principle in physics, is found to be broken down at high energy case [38–40]. The Lorentz dispersion relation is required to be modified in the high energy case and the magnitude of this correction term should be in Planck scale [41–43]. Based on the LIV, the Klein-Gordon equation and Dirac equation are required to modify for curved spacetime [44–47]. This leads to the correction of physical quantities such as black hole quantum tunneling radiation, temperature, entropy and other thermodynamic quantities. Thus the study of tunneling radiation of bosons and fermions under LIV is a promising area of research. In the last few years,

based on LIV modification, many researchers studied the corrected tunneling radiation for different types of black holes [48–56].

Hawking and Page [57] discovered a phase transition between the Schwarzschild-AdS black hole and the thermal AdS space. Chamblin et al. [58] investigated the first order phase transition in Reissner-Nordstrom-AdS (RNAdS) black holes and explored the analogy of phase transition to Van der Waals liquid-gas system both in canonical ensemble and in grand canonical ensemble. Further, treating the cosmological constant as a thermodynamic pressure, $P = -\frac{\Lambda}{8\pi}$ and its conjugate quantity as a thermodynamical volume, the phase transitions and critical behaviors of RNAdS black hole in extended phase space are studied in [59–61]. These phase transitions of RNAdS in the extended phase space are similar to the Van der Waals liquid-gas system's phase transitions. Moreover, the critical exponents are the same with those of Van der Waals liquid-gas system. The $P-V$ criticality of black holes in different modified theories of gravitation are extensively studied in [62–68]. The Van der Waals liquid-gas system analogous to the $P-v$ criticality of charged dynamical (Vaidya) AdS black hole, including the equation of state and critical exponents were studied in [69]. Further Van der Waals like liquid-gas phase transition is observed in the $T-S$ plane of black hole [70].

For Van der Waals liquid-gas system, above the critical temperature T_c the isothermal curve shows a similar behavior to the experimental results but below T_c there exists an oscillating region which violates the condition of stable equilibrium. The theoretical prediction and experimental results are reconciled by substituting the oscillating part of the isotherm with a horizontal isobar that satisfies Maxwell's equal-area law. Ref. [60, 71–73] studied the Maxwell's equal-area law in $P-v$ plane. Further, the construction of Maxwell's equal-area law is extended in $P-V$ and $T-S$ planes [74–78]. However, no research work has been done so far for the construction of Maxwell's equal-area law under LIV modification. Our work is to construct Maxwell's equal-area law under LIV for VBdS black hole in extended phase space.

The organization of the paper is as follows: The correction of quantum tunneling radiation of fermions from VBdS black hole induced by LIV is presented in Section 2. In Section 3, we study the Maxwell equal-area law of VBdS black hole in extended phase space

and obtain the positions of phase transition under LIV modification for different conjugate variables $P - v$, $P - V$ and $T - S$. In Section 4, under LIV modification we present the entropy correction and calculate the modified Helmholtz free energy, internal energy and enthalpy. In Section 5, the stability of the VBdS black hole under LIV is discussed through Gibbs free energy, heat capacity and Hessian matrix. The last section gives the discussions and conclusions.

2. Tunneling of VBdS black hole under LIV

The metric of the nonstationary VBdS black hole in an advanced Eddington-Finkelstein coordinate (v, r, θ, ϕ) is defined by [79]

$$ds^2 = - \left(1 - \frac{2M}{r} + \frac{Q^2}{r^2} - \frac{\Lambda}{3} r^2 \right) dv^2 + 2dv dr + r^2(d\theta^2 + \sin^2 \theta d\phi^2), \quad (1)$$

where v indicates the Eddington time and $M = M(v)$ and $Q = Q(v)$, are the mass and charge of the black hole respectively and Λ is the cosmological constant. The four vector electromagnetic potentials A_μ of VBdS black hole is given by $A_\mu = (\frac{Q}{r}, 0, 0, 0)$. The non zero contravariant components of VBdS black hole are given by

$$g^{11} = \left(1 - \frac{2M}{r} + \frac{Q^2}{r^2} - \frac{\Lambda}{3} r^2 \right), g^{10} = g^{01} = 1, \\ g^{22} = \frac{1}{r^2}, g^{33} = \frac{1}{r^2 \sin^2 \theta}. \quad (2)$$

Since the space-time represented by Eq. (1) is spherically symmetric, the event horizon is necessary a null surface $r_h = r_h(v)$ that satisfies the null hypersurface condition

$$g^{ab} \frac{\partial F}{\partial x^a} \frac{\partial F}{\partial x^b} = 0, \quad (3)$$

with $F(v, r) = 0$. Using Eq. (1) in Eq. (3), the horizon equation and mass of the VBdS black hole are

$$1 - \frac{2M}{r_h} + \frac{Q^2}{r_h^2} - \frac{\Lambda}{3} r_h^2 - 2\dot{r}_h = 0 \quad (4)$$

and

$$M = \frac{r_h}{2} + \frac{Q^2}{2r_h} - r_h \dot{r}_h - \frac{\Lambda r_h^3}{6} \quad (5)$$

respectively where $\dot{r}_h = \frac{dr_h}{dv}$.

2.1. Modified form of Hamilton-Jacobi equation:

Refs. [41, 80–82] investigated a relation in the study of string theory and quantum gravity as

$$\tilde{P}_0^2 = \tilde{P}^2 + m^2 - (\lambda \tilde{P}_0)^i \tilde{P}^2, \quad (6)$$

where \tilde{P} and \tilde{P}_0 represent momentum and energy of the particle with the static mass m . The constant term λ

is in the magnitude of Planck scale which is determined from the LIV theory from Eq. (6). Then, the value of i is unity in the Liouville string theory. A modified form of Dirac equation is determined from Eq. (6) for $i = 2$ [43]. The Rarita-Schwinger-Hamilton-Jacobi equation is given by [48]

$$g^{\mu\nu} (\partial_\mu \Psi + eA_\mu) (\partial_\nu \Psi + eA_\nu) + m^2 - 2\lambda m (\partial_v \Psi + eA_0) \\ g^{0i} \partial_i \Psi - \lambda^2 [(\partial_v \Psi + eA_0) g^{0j} \partial_j \Psi]^2 = 0, \quad (7)$$

where $\mu, \nu = 0, 1, 2, 3$ and $i, j = 1, 2, 3$. The action of the fermion can be obtained from Eq. (7) and corresponding modified Hawking temperature of VBdS black hole can be calculated. Eq. (7) gives a highly accurate dynamic equation due to presence of the term $O(\lambda^2)$ and the involvement of LIV. Using Eq. (2) in Eq. (7) we get

$$\frac{\Delta}{r^2} \left(\frac{\partial \Psi}{\partial r} \right)^2 + \frac{1}{r^2} \left(\frac{\partial \Psi}{\partial \theta} \right)^2 + \frac{1}{r^2 \sin^2 \theta} \left(\frac{\partial \Psi}{\partial \phi} \right)^2 \\ + 2 \left(\frac{\partial \Psi}{\partial v} + eA_0 \right) \left(\frac{\partial \Psi}{\partial r} \right) - 2\lambda m \left(\frac{\partial \Psi}{\partial v} + eA_0 \right) \left(\frac{\partial \Psi}{\partial r} \right) \\ - \lambda^2 \left(\frac{\partial \Psi}{\partial v} + eA_0 \right)^2 \left(\frac{\partial \Psi}{\partial r} \right)^2 = 0, \quad (8)$$

where $\Delta = r^2 - 2Mr + Q^2 - \frac{\Lambda}{3} r^4$. Since the action Ψ involved in the above equation is a function of coordinates v, r, θ, ϕ , the action Ψ can be derived by using the tortoise coordinate transformation. Therefore the tortoise coordinate transformation is defined by

$$r_* = r + \frac{1}{2\kappa} \ln \frac{r - r_h(v)}{r_h(v_0)}, \\ v_* = v - v_0, \quad (9)$$

where κ and $r_h(v)$ are the surface gravity and location of event horizon respectively. v_0 is the initial time where the fermions gets out across the event horizon. The tortoise coordinate transformation describes the spacetime geometry outside the event horizon of VBdS black hole. In this case, r_* approaches to negative infinity near the event horizon of VBdS black hole and r_* approaches to positive infinity when tending to infinite point. Eq. (9) can be written as

$$\frac{\partial}{\partial r} = \frac{1 + 2\kappa(r - r_h)}{2\kappa(r - r_h)} \frac{\partial}{\partial r_*}, \\ \frac{\partial}{\partial v} = \frac{\partial}{\partial v_*} - \frac{\dot{r}_h}{2\kappa(r - r_h)} \frac{\partial}{\partial r_*}. \quad (10)$$

To study modified Hawking temperature, the action S can be defined as

$$\Psi = R(v_*, r_*) + X(\theta, \phi), \quad (11)$$

and let

$$\frac{\partial R}{\partial v_*} = \frac{\partial \Psi}{\partial v_*} = -\omega, \quad (12)$$

where ω is energy of the particle. Using Eqs. (9)-(12) in Eq. (8), we get

$$\begin{aligned} & \frac{1}{2\kappa(r-r_h)} \left[\frac{\Delta}{r^2} (1+2\kappa(r-r_h))^2 - 2\dot{r}_h(1+2\kappa(r-r_h)) \right. \\ & \quad \left. + 2\lambda m \dot{r}_h(1+2\kappa(r-r_h)) - \lambda^2 \left(\frac{\partial R}{\partial v_*} + eA_0 \right)^2 \right. \\ & \quad \left. (1+2\kappa(r-r_h))^2 \right] \left(\frac{\partial R}{\partial r_*} \right)^2 + 2 \left(\frac{\partial R}{\partial v_*} + eA_0 \right) \\ & \quad (1-\lambda m)(1+2\kappa(r-r_h)) \left(\frac{\partial R}{\partial r_*} \right) + 2\kappa(r-r_h) \\ & \quad [m^2 + o(\lambda^2)] = 0. \end{aligned} \quad (13)$$

To obtain the first order term of λ in the final outcome, multiplying both sides of the above equation by $2\kappa(r-r_h)$ and taking the limit as $r \rightarrow r_h$, we get

$$\left(\frac{\partial R}{\partial r_*} \right)^2 - 2(1-\lambda m)(\omega - \omega_0) \left(\frac{\partial R}{\partial r_*} \right) = 0, \quad (14)$$

where $\omega_0 = eQ/r_h$. To derive the surface gravity near the horizon of VBdS black hole, the limiting value of the coefficient $\left(\frac{\partial R}{\partial r_*} \right)^2$ is taken as unity

$$\begin{aligned} & \lim_{\substack{r \rightarrow r_h \\ v \rightarrow v_0}} \frac{1}{2\kappa(r-r_h)r^2} \left[\Delta[1+2\kappa(r-r_h)] - 2r^2\dot{r}_h + \right. \\ & \quad \left. 2\lambda m r^2 \dot{r}_h - \lambda^2 r^2 (\omega - \omega_0)^2 \{1+2\kappa(r-r_h)\} \right] = 1. \end{aligned} \quad (15)$$

From the above equation, the surface gravity κ is calculated as

$$\begin{aligned} \kappa &= \frac{1}{2(1-2\dot{r}_h)r_h^3} \\ & \quad \times \left[r_h^2 - Q^2 - \Lambda r_h^4 - 2r_h^2 \dot{r}_h(1+2\lambda m) \right]. \end{aligned} \quad (16)$$

Using Eq. (10) in Eq. (14), we get

$$\begin{aligned} \frac{\partial R}{\partial r} &= \frac{1+2\kappa(r-r_h)}{2\kappa(r-r_h)} (1-\lambda m) \\ & \quad [(\omega - \omega_0) \pm (\omega - \omega_0)]. \end{aligned} \quad (17)$$

Integrating Eq. (17) by applying Feynman prescription near the horizon of black hole, we get

$$R_{\pm} = \frac{\pi i}{2\kappa} (1-\lambda m) [(\omega - \omega_0) \pm (\omega - \omega_0)], \quad (18)$$

where R_+ and R_- are the outgoing and ingoing waves respectively near the event horizon of black hole. The tunneling probability of fermions is calculated near the event horizon of VBdS black hole in accordance with semiclassical approximation as

$$\begin{aligned} \Gamma &= \exp(-2Im\Psi) = \exp(-2Im R_{\pm}) \\ &= \exp \left[-\frac{2\pi(\omega - \omega_0)}{\kappa_0} \right] \\ &= \exp \left(-\frac{\omega - \omega_0}{T} \right), \end{aligned} \quad (19)$$

where $\kappa_0 = \kappa/(1-\lambda m)$ represents the modified surface gravity of VBdS black hole due to Lorentz invariance theory. Since Eq. (19) is similar to Boltzmann formula, the Hawking temperature of the black hole is derived as

$$\begin{aligned} T &= \frac{\kappa_0}{2\pi} \\ &= \frac{r_h - M - 2r_h \dot{r}_h(1+m\lambda) - \lambda^2(\omega - \omega_0)^2 r_h - \frac{2\Lambda}{3} r_h^3}{2\pi[2Mr_h - Q^2 + \lambda^2(\omega - \omega_0)^2 r_h^2 + \frac{\Lambda}{3} r_h^4](1-\lambda m)}. \end{aligned} \quad (20)$$

It is noted from Eq. (20) that the Hawking temperature and tunneling rate of VBdS black hole have been modified due to presence of correction term λ . Applying binomial expansion for $(1-\lambda m)^{-1}$ and ignoring higher power of λ , Eq. (20) can be written as

$$T = T_h + \frac{\lambda m}{4\pi r_h(1-2\dot{r}_h)} \left(1 - \frac{Q^2}{r_h^2} - \Lambda r_h^2 - 3\dot{r}_h \right), \quad (21)$$

where T_h is the original Hawking temperature of VBdS black hole in the absence of the LIV theory which is given by

$$T_h = \frac{1 - \frac{Q^2}{r_h^2} - \Lambda r_h^2 - 2\dot{r}_h}{4\pi r_h(1-2\dot{r}_h)}. \quad (22)$$

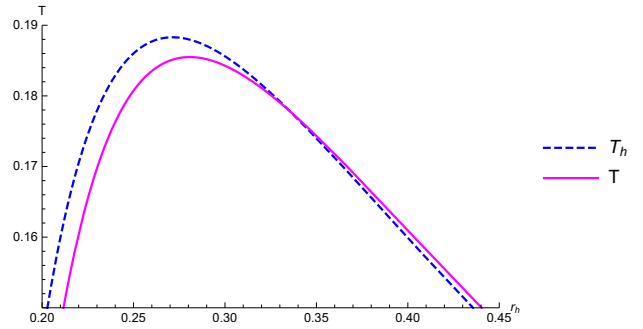


Figure 1. Original and modified Hawking temperature of VBdS black hole versus radius of event horizon r_h for $Q = 0.1$, $\lambda = 1$, $\Lambda = 0.1$, $m = 0.1$ and $\dot{r}_h = 0.3$.

In our analysis, we consider the cosmological constant Λ as a thermodynamic pressure P

$$P = -\frac{\Lambda}{8\pi}. \quad (23)$$

Since $\Lambda > 0$ in de Sitter space, P is negative. Although, it is more appropriate to take P as a tension than a pressure, we shall continue to refer to it as pressure. Refs. [61, 64, 83, 84] studied the thermodynamics of de Sitter black holes by treating the positive cosmological constant as thermodynamic pressure. Further the corresponding conjugate thermodynamic volume is given as

$$V = \frac{4}{3}\pi r_h^3. \quad (24)$$

3. Equal area law of VBdS black hole in extended phase space

In this section, we will investigate the corresponding Maxwell's equal-area law of VBdS black hole under LIV theory. The equation of state of the VBdS black hole under LIV theory may be obtained from Eq. (21) and can be written as $f(T, P, V) = 0$. We construct the phase transition of VBdS black hole in $P - \tilde{v}$, $P - V$ and $T - S$ respectively based on Maxwell's equal-area law.

3.1. Construction of the equal-area law in $P - \tilde{v}$ diagram

The equation of state for the VBdS black hole under LIV theory is obtained from Eq. (21) as

$$P = \frac{T(1 - 2\dot{r}_h)}{2r_h(1 + m\lambda)} + \frac{Q^2}{8\pi r_h^4} - \frac{\Sigma}{8\pi r_h^2(1 + m\lambda)}. \quad (25)$$

where $\Sigma = 1 + \lambda m - 2\dot{r}_h - 3\lambda m\dot{r}_h$. The equation of state reduces to

$$P = \frac{T(1 - 2\dot{r}_h)}{\tilde{v}(1 + m\lambda)} + \frac{2Q^2}{\pi\tilde{v}^4} - \frac{\Sigma}{2\pi\tilde{v}^2(1 + m\lambda)}, \quad (26)$$

where $\tilde{v} = 2r_h$ is the specific volume. Eq. (26) is used to illustrate $P - \tilde{v}$ curves at constant Q for a given temperature T .

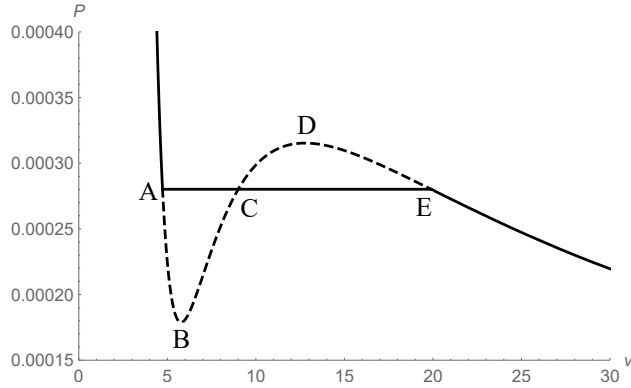


Figure 2. $P - \tilde{v}$ diagram below the critical temperature T_c . Here we set $m = 0.1$, $Q = 1$, $r_h = 0.3$ and $\lambda = 0.1$.

From the Fig. 2, we observe that there is a phase where one value of the pressure P corresponds to three different values of \tilde{v} in the isothermal curves below the critical temperature T_c . Experiment results show that there should be a horizontal isobar in the isotherm to represent the condensation line where the gas coexists with the liquid.

The thermodynamic system's chemical potential should satisfy

$$d\mu = -SdT + VdP. \quad (27)$$

In the isotherm transformation, the difference of chemical potential between two states with the pressure P and P_0 should be

$$\mu - \mu_0 = \int_{P_0}^P VdP. \quad (28)$$

From Fig. 2, it is noted that the black hole is in the “gas” phase at point E. But the black hole is entirely in the “liquid” phase at point “A.” Furthermore, the region between A and E may be considered as a coexistence phase. Since the segment BD defies the equilibrium criteria, the oscillating portion of the curve between A and E cannot be the coexistence line. The chemical potentials are the same at points A and E, which is the thermodynamic condition for phase equilibrium. From Eq. (28) we get

$$\int_{EDCBA} \tilde{v} dP = 0, \quad (29)$$

showing that area ABC is equal to area CDE.

We will find the position of the points A and E for VBdS black hole under LIV and will also discuss the effect caused by Lorentz invariance violation parameter λ .

The specific volumes at the boundary of the two-phase coexistence area with a temperature $T_0 < T_c$ are \tilde{v}_1 and \tilde{v}_2 respectively for the VBdS black hole. The corresponding equal area isobar $P = P_0$, is defined by the event horizon radius r_h and is smaller than the critical pressure P_c . Thus, from Maxwell's equal area law, we have

$$\begin{aligned} P_0(\tilde{v}_2 - \tilde{v}_1) &= \int_{\tilde{v}_1}^{\tilde{v}_2} P d\tilde{v} \\ &= \int_{r_1}^{r_2} \left(\frac{T_0(1 - 2\dot{r}_h)}{2r(1 + m\lambda)} + \frac{Q^2}{8\pi r^4} - \frac{\Sigma}{8\pi r^2} \right) \times 2dr. \end{aligned} \quad (30)$$

Then we can obtain

$$\begin{aligned} 2P_0(r_2 - r_1) &= \frac{T_0(1 - 2\dot{r}_h)}{(1 + m\lambda)} \ln\left(\frac{r_2}{r_1}\right) - \frac{Q^2}{12\pi} \left(\frac{1}{r_2^3} - \frac{1}{r_1^3} \right) \\ &\quad + \frac{\Sigma}{4\pi(1 + m\lambda)} \left(\frac{1}{r_2} - \frac{1}{r_1} \right). \end{aligned} \quad (31)$$

From Eq. (25), we have

$$P_0 = \frac{T_0(1 - 2\dot{r}_h)}{2r_1(1 + m\lambda)} + \frac{Q^2}{8\pi r_1^4} - \frac{\Sigma}{8\pi r_1^2} \quad (32)$$

and

$$P_0 = \frac{T_0(1 - 2\dot{r}_h)}{2r_2(1 + m\lambda)} + \frac{Q^2}{8\pi r_2^4} - \frac{\Sigma}{8\pi r_2^2}, \quad (33)$$

where r_1 and r_2 are the event horizon radii of the \tilde{v}_1 and \tilde{v}_2 respectively.

From Eqs. (32) and (33) and setting $x = \frac{r_1}{r_2}$, we get

$$0 = \frac{T_0(1-2r_h)}{(1+m\lambda)} + \frac{Q^2(1+x)(1+x^2)}{4\pi x^3 r_2^3} - \frac{\Sigma(1+x)}{4\pi r_2 x(1+m\lambda)} \quad (34)$$

and

$$2P_0 = \frac{T_0(1-2r_h)(1+x)}{2r_2 x(1+m\lambda)} + \frac{Q^2(1+x^4)}{8\pi x^4 r_2^4} - \frac{\Sigma(1+x^2)}{8\pi r_2^2 x^2(1+m\lambda)}. \quad (35)$$

Eq. (31) can be written as

$$2P_0 = \frac{Q^2(1+x+x^2)}{12\pi x^3 r_2^4} - \frac{\Sigma}{4\pi x r_2^2(1+m\lambda)} - \frac{T_0 \ln x(1-2r_h)}{r_2(1+m\lambda)(1-x)}. \quad (36)$$

From Eqs. (35) and (36), we find that

$$\frac{4\pi r_2 x T_0(1-2r_h)(1-x^2+2x \ln x) - \Sigma(1-x)^3}{(x-1)(1+m\lambda)} = \frac{Q^2(1-x)^2(3x^2+4x+3)}{3r_2^2 x^2}. \quad (37)$$

Utilizing Eq. (34) in Eq. (37), we find

$$r_2^2 = \frac{Q^2(1+m\lambda)}{3\Sigma} \times \frac{y_1(x)}{y_2(x)}, \quad (38)$$

where

$$y_1(x) = 4 - 4x^3 + 3(1+x+x^2+x^3) \ln x$$

and $y_2(x) = x^2[2 - 2x + (1+x) \ln x]$.

When $x \rightarrow 1$, we must have $r_1 = r_2 = r_c$. Therefore from Eq. (38), we obtain

$$r_c^2 = \frac{Q^2(1+m\lambda)}{3\Sigma} \lim_{x \rightarrow 1} \frac{y_1(x)}{y_2(x)}. \quad (39)$$

By using L'Hopital rule, Eq. (39) becomes

$$r_c = \left\{ \frac{6Q^2(1+m\lambda)}{\Sigma} \right\}^{\frac{1}{2}}. \quad (40)$$

It follows that

$$\tilde{v}_c = \frac{2Q\sqrt{6(1+m\lambda)}}{\sqrt{\Sigma}} \quad (41)$$

$$T_c = \frac{\Sigma^{\frac{3}{2}}}{3\sqrt{6}\pi Q(1-2r_h)\sqrt{1+m\lambda}}. \quad (42)$$

Substituting the value of r_2 in Eq. (34) and taking $T_0 = \chi T_c$, we can obtain

$$2\sqrt{2}\chi x^3 \left(\frac{y_1(x)}{y_2(x)} \right)^{\frac{3}{2}} = 9(1+x) \left[x^2 \frac{y_1(x)}{y_2(x)} - 3x^2 - 3 \right]. \quad (43)$$

We plot the pressure P in terms of specific volume

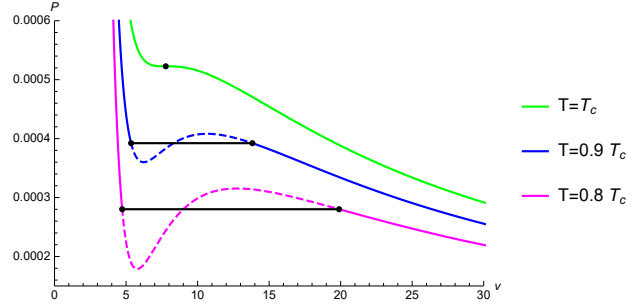


Figure 3. The simulated phase transition (black solid lines) and the boundary of a two phase coexistence on the base of isobar in the $P-v$ diagram for VBdS black hole under LIV theory with $m = 0.1$, $Q = 1$, $r_h = 0.3$ and $\lambda = 0.1$. The temperature of isotherms decreases from top to bottom.

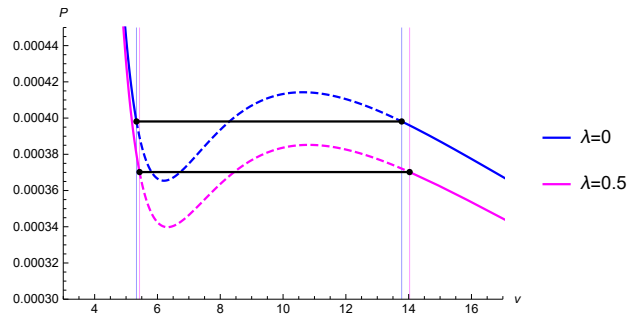


Figure 4. The simulated phase transition (black solid lines) and the boundary of a two phase coexistence for $T < T_c$ in the $P-\tilde{v}$ diagram for (a) $\lambda = 0$ (top) and (b) $\lambda = 0.5$ (bottom) with fixed $m = 0.1$, $Q = 1$ and $r_h = 0.3$.

\tilde{v} for different values of T and λ in Figs. 3 and 4 respectively and also show simulated phase transition and the boundary of a two-phase coexistence on the base of isotherms in the $P-\tilde{v}$ diagram. From Fig. 3, it is noted that when the temperature increases, the isobar in the isotherm becomes shorter. The boundary of the isobar coincides when the temperature reaches its critical value. Moreover, from Fig. 4, we observe that under the influence of LIV theory, the phase transition process becomes longer. Further, comparing the original and modified pressure, it is noted that the

Table 1. Numerical solutions for x , r_1 , r_2 , \tilde{v}_1 , \tilde{v}_2 and P_0 for different values of λ with $m = 0.1$, $Q = 1$ and $r_h = 0.3$.

λ	χ	x	r_1	r_2	v_1	v_2	P_0
0	1	1	3.87298	3.87298	7.74597	7.74597	0.000530516
	0.9	0.386969	2.66568	6.88861	5.33135	13.7772	0.000398128
	0.8	0.237789	2.35641	9.90968	4.71283	19.8194	0.000284384
0.1	1	1	3.88744	3.88744	7.77489	7.77489	0.000522667
	0.9	0.386969	2.67563	6.91433	5.35126	13.8287	0.000392237
	0.8	0.237789	2.36521	9.94668	4.73043	19.8934	0.000280176
0.5	1	1	3.94405	3.94405	7.88811	7.88811	0.000493299
	0.9	0.386969	2.71459	7.01501	5.42919	14.03	0.000370198
	0.8	0.237789	2.39966	10.0915	4.79931	20.1831	0.000264433

phase transition occurs at a lower pressure due to LIV theory.

The numerical values of x , r_1 , r_2 , \tilde{v}_1 , \tilde{v}_2 and P_0 for different values of λ for VBdS black hole under LIV theory are displayed in Table 1. From Table 1, we observe that the values of x decrease as the values of χ decrease, but λ has no effect on it. The values of r_2 and \tilde{v}_2 increase with increasing λ but decrease with increasing χ . However, the values of P_0 decreases with increasing λ but its value increases with increasing χ .

3.2. Equal-area law in $P - V$ diagram

This subsection examines the condition in which the conjugate variables (P , V) occur under Maxwell's equal area law. Further, we will discuss the phase transition of VBdS black hole in $P - V$ diagram based on Maxwell's equal-area law. On the isotherm with temperature T_0 ($T_0 < T_c$) in $P - V$ diagram, there exist two points (P_0, V_1) and (P_0, V_2) satisfying Maxwell's equal area law,

$$P_0(V_2 - V_1) = \int_{V_1}^{V_2} P dV = \int_{r_1}^{r_2} \left(\frac{T_0(1 - 2r_h)}{2r(1 + m\lambda)} + \frac{Q^2}{8\pi r^4} - \frac{\Sigma}{8\pi r^2} \right) \times 4\pi r^2 dr. \quad (44)$$

From Eq. (44), one can derive the relation

$$2P_0 = \frac{3Q^2}{4\pi r_2^4 x(1 + x + x^2)} + \frac{3T_0(1 + x)(1 - 2r_h)}{2r_2(1 + \lambda m)(1 + x + x^2)} - \frac{3\Sigma}{4\pi r_2^2(1 + x + x^2)(1 + \lambda m)}. \quad (45)$$

Similarly we can obtain

$$r_2^2 = \frac{Q^2(1 + 4x + x^2)(1 + \lambda m)}{\Sigma x^2}. \quad (46)$$

Taking $T_0 = \chi T_c$, when $0 < \chi < 1$, we get

$$\chi = \frac{3\sqrt{6}x(1 + x)}{(1 + 4x + x^2)^{3/2}}. \quad (47)$$

The critical state is obtained when $x \rightarrow 1$ i.e. $\chi \rightarrow 1$. Using Eqs. (46) and (45), we can solve

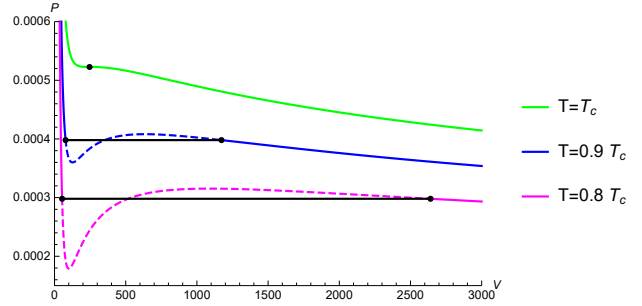


Figure 5. The simulated phase transition (black solid lines) and the boundary of a two phase coexistence on the base of isobar in the $P - V$ diagram for VBdS black hole under LIV theory with $m = 0.1$, $Q = 1$, $r_h = 0.3$ and $\lambda = 0.1$. The temperature of isotherms decrease from top to bottom.

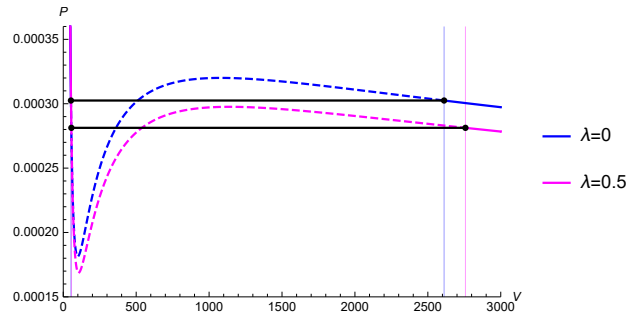


Figure 6. The simulated phase transition (black solid lines) and the boundary of a two phase coexistence for $T < T_c$ in the $P - V$ diagram for (a) $\lambda = 0$ (top) and (b) $\lambda = 0.5$ (bottom) with fixed $m = 0.1$, $Q = 1$ and $r_h = 0.3$.

r_2 and P_0 for different values of λ and a fixed χ by deriving a specific value of x from Eq. (47). Using the values of r_2 , we can find the values of r_1 and the corresponding values of V_1 and V_2 can be obtained. To investigate the impact of parameter λ on phase transition processes, by fixing the parameters $m = 0.1$, $Q = 1$, $r_h = 0.3$ and $\chi = 0.8, 0.9, 1$, the values of r_1 , r_2 , V_1 , V_2 and P_0 are obtained. The results are shown in Table 2. From Table 2, it is shown that x is not related to the LIV parameter λ . Increasing the values of λ , the values of r_2 and v_2 increase but increasing the

values of χ , the values of r_2 and v_2 decrease. Further, P_0 reduces with increasing λ implying that the LIV theory lowers the pressure of phase transition. We plot $P - V$ daigram for different values of χ and λ in Figs. 5 and 6 respectively and show the isobar representing the process of isothermal phase transition or the two-phase coexistence situation like that of Van der Waals system. Fig. 5 shows that as the temperature increases the isothermal phase transition process becomes shorter and when the temperature reaches its critical temperature, it turns into a single point. Further, from Fig. 6 we observe that the isothermal phase transition process becomes longer under the influence of LIV theory. Moreover, the isobar representing the two phase coexistence occurs at lower pressure under the influence of Lorentz invariance violation theory.

3.3. Equal-area law in $T - S$ diagram

In this section, through Maxwell's equal-area law, we will construct the phase transition in $T - S$ for the VBdS black hole under LIV theory. The equation of state of Eq. (25) can be written as

$$T = \frac{2P\sqrt{S}(1+\lambda m)}{\sqrt{\pi}(1-2\dot{r}_h)} + \frac{\Sigma}{4\sqrt{\pi S}(1-2\dot{r}_h)} - \frac{Q^2\sqrt{\pi}(1+\lambda m)}{4S^{\frac{3}{2}}(1-2\dot{r}_h)}, \quad (48)$$

where $S = \pi r_h^2$ is the Bekenstein-Hawking entropy.

For a given charge Q , LIV parameter λ and pressure $P_0 < P_c$, the entropy at the boundary of the two-phase coexistence region are S_1 and S_2 respectively and their corresponding temperature is T_0 ($T_0 \leq T_c$). It is worth mentioning that the temperature depends on the horizon radius r_h . From Maxwell's equal area law, we have

$$\begin{aligned} T_0(S_2 - S_1) &= \int_{S_1}^{S_2} T dS \\ &= \int_{r_1}^{r_2} \frac{2Pr(1+\lambda m)}{1-2\dot{r}_h} + \frac{\Sigma}{4\pi r_h(1-2\dot{r}_h)} \\ &\quad - \frac{Q^2(1+\lambda m)}{4\pi r_h^3(1-2\dot{r}_h)} \times 2\pi r_h dr_h. \end{aligned} \quad (49)$$

Then one can derive

$$\begin{aligned} 2\pi T_0 &= \frac{-Q^2(1+\lambda m)}{x(1+x)(1-2\dot{r}_h)r_2^3} + \frac{\Sigma}{(1+x)(1-2\dot{r}_h)r_2} \\ &\quad + \frac{8\pi P_0 r_2(1+\lambda m)(1+x+x^2)}{3(1+x)(1-2\dot{r}_h)}, \end{aligned} \quad (50)$$

$$T_0 = \left[\frac{-Q^2(1+\lambda m)}{4\pi r_1^3(1-2\dot{r}_h)} + \frac{2P_0 r_1(1+\lambda m)}{1-2\dot{r}_h} + \frac{\Sigma}{4\pi r_1(1-2\dot{r}_h)} \right] \quad (51)$$

and

$$T_0 = \left[\frac{-Q^2(1+\lambda m)}{4\pi r_2^3(1-2\dot{r}_h)} + \frac{2P_0 r_2(1+\lambda m)}{1-2\dot{r}_h} + \frac{\Sigma}{4\pi r_2(1-2\dot{r}_h)} \right]. \quad (52)$$

From Eqs. (51) and (52), we obtain the following equations

$$\begin{aligned} &\frac{Q^2(1+\lambda m)(1+x+x^2)}{x^3 r_2^3} + 8\pi P_0(1+\lambda m)r_2 \\ &- \frac{\Sigma}{x r_2} = 0 \end{aligned} \quad (53)$$

and

$$\begin{aligned} 8\pi T_0 &= \frac{-Q^2(1+\lambda m)(1+x^3)}{(1-2\dot{r}_h)x^3 r_2^3} + \frac{\Sigma(1+x)}{(1-2\dot{r}_h)x r_2} \\ &\quad + \frac{8\pi P_0 r_2(1+\lambda m)(1+x)}{(1-2\dot{r}_h)}. \end{aligned} \quad (54)$$

Using Eqs. (50) and (54), we can derive the relation

$$\begin{aligned} 8\pi P_0 r_2(1+\lambda m) &= \frac{-3Q^2(1+3x+x^2)(1+\lambda m)}{r_2^3 x^3} \\ &\quad + \frac{3\Sigma}{r_2 x}. \end{aligned} \quad (55)$$

Using Eq. (55), Eq. (53) reduces to

$$r_2^2 = \frac{Q^2(1+4x+x^2)(1+\lambda m)}{\Sigma x^2}. \quad (56)$$

From Eq. (53), we obtain

$$P_0 = \frac{3x^2 \Sigma^2}{8\pi Q^2(1+4x+x^2)^2(1+\lambda m)^2}. \quad (57)$$

The critical radius $r_c = r_1 = r_2$ and critical pressure P_c are obtained as follows

$$r_c = \frac{\sqrt{6}Q(1+\lambda m)^{\frac{1}{2}}}{\Sigma^{\frac{1}{2}}} \quad (58)$$

and

$$P_c = \frac{\Sigma^2}{96\pi Q^2(1+\lambda m)^2}. \quad (59)$$

Taking $P_0 = \chi P_c$, when $0 < \chi < 1$ we get

$$\chi = \frac{36x^2}{(1+4x+x^2)^2}. \quad (60)$$

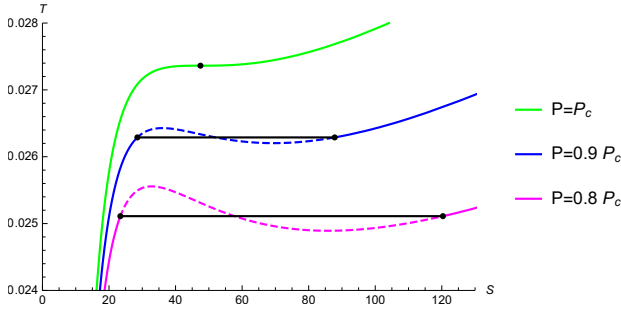
We plot $T - S$ diagrams for different values of χ and λ in Figs. 7 and 8 respectively and show the isotherms (black solid lines) which represent the simulated phase transition processes derived from Maxwell's equal area law. From Fig. 7, we observe that the isotherm becomes shorter with increasing the pressure and once the pressure reaches its critical point it converges to a point. For Fig. 8, we take $P < P_c$ and plot the $T - S$ diagrams for $\lambda = 0$ and 0.5. It is noticed that the phase transition process for $\lambda = 0.5$ is longer than that of $\lambda = 0$ which implies the LIV theory increases the phase transition process. We

Table 2. Numerical solutions for x , r_1 , r_2 , V_1 , V_2 and P_0 for different values of λ with $m = 0.1$, $Q = 1$ and $r_h = 0.3$.

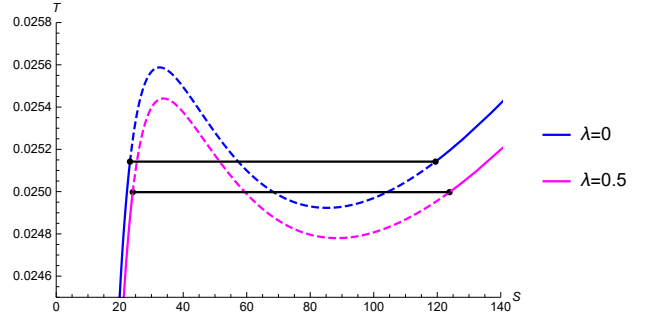
λ	χ	x	r_1	r_2	V_1	V_2	P_0
0	1	1	3.87298	3.87298	243.347	243.347	0.000530516
	0.9	0.404703	2.63752	6.51716	76.8554	1159.48	0.000403993
	0.8	0.272204	2.32535	8.5427	52.6691	2611.4	0.000302491
0.1	1	1	3.88744	3.88744	246.083	246.083	0.000522667
	0.9	0.404703	2.64736	6.5415	77.7194	1172.52	0.000398015
	0.8	0.272204	2.3304	8.5746	53.2613	2640.76	0.000298015
0.5	1	1	3.94405	3.94405	256.99	256.99	0.000493299
	0.9	0.404703	2.68592	6.63675	81.1644	1224.49	0.000375652
	0.8	0.272204	2.36803	8.69946	55.6221	2757.82	0.00028127

Table 3. Numerical solutions for x , r_1 , r_2 , S_1 , S_2 and T_0 for different values of λ with $m = 0.1$, $Q = 1$ and $r_h = 0.3$.

λ	χ	x	r_1	r_2	S_1	S_2	T_0
0	1	1	3.87298	3.87298	47.1239	47.1239	0.0273958
	0.9	0.569919	3.00187	5.26719	28.3095	87.158	0.0263212
	0.8	0.441089	2.7198	6.16609	23.2393	119.445	0.0251419
0.1	1	1	3.88744	3.88744	47.4764	47.4764	0.0273621
	0.9	0.569919	3.01307	5.28685	28.5213	87.81	0.0262889
	0.8	0.441089	2.72995	6.18911	23.4131	120.339	0.0025111
0.5	1	1	3.94405	3.94405	48.8692	48.8692	0.0272384
	0.9	0.569919	3.05695	5.36384	29.358	90.386	0.02617
	0.8	0.441089	2.76971	6.27924	24.1	123.869	0.0249975

**Figure 7.** The simulated phase transition (black solid lines) and the boundary of a two phase coexistence on the base of isobaric in the $T - S$ diagram for VBdS black hole under LIV theory with $m = 0.1$, $Q = 1$, $r_h = 0.3$ and $\lambda = 0.1$. The pressure of isotherms decreases from top to bottom.

compute the values of x , r_1 , r_2 , S_1 , S_2 and T_0 as $\chi = 0.8, 0.9, 1$ and $\lambda = 0, 0.1, 0.5$, respectively in order to determine the influence of these parameters on the simulated phase transition process and the two-phase coexistence region. The tabulated values are displayed in Table 3. Here, x is unrelated to λ . r_2 and S_2 are directly proportional to λ but they are inversely proportional to χ . Moreover, T_0 is inversely proportional to λ and directly proportional to χ . Both r_2 and S_2 increase with increasing λ but decrease with increasing χ . However, T_0 decreases with increasing λ but increases with increasing χ .

**Figure 8.** The simulated phase transition (black solid lines) and the boundary of a two phase coexistence for $P < P_c$ in the $T - S$ diagram for (a) $\lambda = 0$ (top) and (b) $\lambda = 0.5$ (bottom) with fixed $m = 0.1$, $Q = 1$ and $r_h = 0.3$.

4. Thermal Fluctuations

In this section, we will evaluate the corrected entropy under the influence of LIV theory. To find the corrected entropy, we use the partition function is considered as [85, 86]

$$\tilde{Z}(\beta) = \int_0^\infty \rho(\tilde{E}) e^{-\beta \tilde{E}} d\tilde{E}, \quad (61)$$

where $\beta = T^{-1}$. Here \tilde{E} and $\rho(\tilde{E})$ are the average energy and quantum density of the system respectively. We apply the inverse Laplace transformation to find

the quantum density as

$$\begin{aligned}\rho(\tilde{E}) &= \frac{1}{2\pi i} \int_{\beta_0-i\infty}^{\beta_0+i\infty} e^{\beta\tilde{E}} \tilde{Z}(\beta) d\beta \\ &= \frac{1}{2\pi i} \int_{\beta_0-i\infty}^{\beta_0+i\infty} e^{\tilde{S}(\beta)} d\beta,\end{aligned}\quad (62)$$

where $\tilde{S} = \ln(\tilde{Z}) + \beta\tilde{E}$ is the corrected entropy for the black hole.

Using steepest descent method at the saddle point β_0 , the complex integral is calculated such that $\left(\frac{\partial\tilde{S}(\beta)}{\partial\beta}\right)_{\beta_0} = 0$ and $\frac{\partial^2\tilde{S}}{\partial\beta^2} > 0$. Further expanding $\tilde{S}(\beta)$ around the equilibrium $\beta = \beta_0$, we have

$$\begin{aligned}\tilde{S}(\beta) &= S + \frac{1}{2}(\beta - \beta_0)^2 \left(\frac{\partial^2\tilde{S}(\beta)}{\partial\beta^2}\right)_{\beta_0} \\ &\quad + \text{higher order terms},\end{aligned}\quad (63)$$

where $S = \tilde{S}$ is the zero-order entropy and satisfies the relation $\frac{\partial S}{\partial\beta} = 0$ and $\frac{\partial^2 S}{\partial\beta^2} = 0$ at $\beta = \beta_0$. From Eqs. (62) and (63), one can derive

$$\rho(\tilde{E}) = \frac{e^S}{2\pi i} \int_{\beta_0-i\infty}^{\beta_0+i\infty} e^{\frac{1}{2}(\beta-\beta_0)^2 \frac{\partial^2\tilde{S}}{\partial\beta^2}} d\beta. \quad (64)$$

The expression of quantum density can be further simplified as

$$\rho(\tilde{E}) = \frac{e^S}{\sqrt{2\pi}} \left(\frac{\partial^2\tilde{S}}{\partial\beta^2}\right)^{-\frac{1}{2}}. \quad (65)$$

Ignoring the higher order terms and after simplification, we obtain

$$\tilde{S} = S - \frac{1}{2} \ln(ST^2). \quad (66)$$

Using the modified Hawking temperature under the influence of LIV theory (T) and the entropy (S) in Eq. (66), we obtain the corrected entropy under the influence of LIV theory as

$$\tilde{S} = \pi r_h^2 + \ln \left[\frac{4\sqrt{\pi}(1-2\dot{r}_h)}{(\Sigma - \Lambda r_h^2(1+\lambda m)) - Q^2(1+\lambda m)r_h^{-2}} \right]. \quad (67)$$

The corrected entropy in the absence of LIV theory S_c is calculated using $T = T_h$ as

$$S_c = \pi r_h^2 + \ln \left[\frac{4\sqrt{\pi}r_h^2(1-2\dot{r}_h)}{-Q^2 + r_h^2(1-2\dot{r}_h - \Lambda r_h^2)} \right]. \quad (68)$$

We plot the original entropy S , corrected entropy in

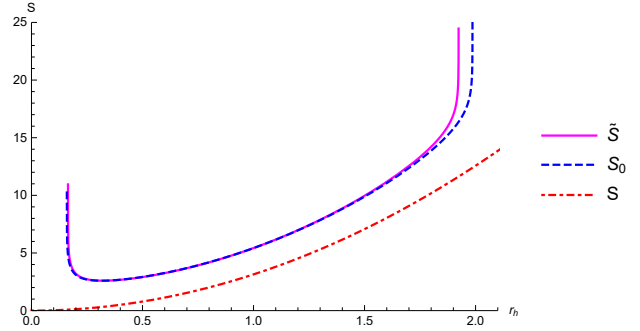


Figure 9. Plot for original entropy, corrected entropy in the absence of LIV theory and corrected entropy under the influence of LIV theory for $Q = 0.1$, $\Lambda = 0.1$, $m = 0.1$ and $r_h = 0.3$.

the absence of LIV theory S_c and corrected entropy under the influence of LIV theory \tilde{S} in Fig. 9. The original entropy (S) is monotonically increasing with radius of event horizon r_h . But S_c and \tilde{S} initially decrease and later keep on increasing. The LIV theory doesn't have much impact in small black hole but in the case of larger black hole LIV theory increases the entropy of black holes.

4.1. Helmholtz free energy

We analyze the behaviour of Helmholtz free energy of VBdS black hole under the influence of LIV theory. The Helmholtz free energy is given by [87]

$$F = - \int \tilde{S} dT. \quad (69)$$

Using Eqs. (21) and (67), we obtain the expression of Helmholtz free energy under the influence of LIV theory as

$$\begin{aligned}F &= \frac{1}{12\pi r_h^3(1-2\dot{r}_h)} \left[Q^2(2+9\pi r_h^2)(1+\lambda m) \right. \\ &\quad \left. + \pi r_h^6(1+\lambda m)\Lambda + 3r_h^4 \left\{ (\pi\Sigma + 2\Lambda(1+\lambda m)) \right\} \right. \\ &\quad \left. - 3 \left\{ r_h^2(\Sigma - \Lambda r_h^2(1+\lambda m)) - Q^2(1+\lambda m) \right\} \right. \\ &\quad \left. \times \ln \left(\frac{4\sqrt{\pi}(1-2\dot{r}_h)}{(\Sigma - \Lambda r_h^2(1+\lambda m)) - Q^2(1+\lambda m)r_h^{-2}} \right) \right].\end{aligned}\quad (70)$$

The Helmholtz free energy without the influence of LIV theory is

$$\begin{aligned}F_0 &= \frac{1}{12\pi r_h^3(1-2\dot{r}_h)} \left[Q^2(2+9\pi r_h^2) + \pi r_h^6\Lambda \right. \\ &\quad \left. + 3r_h^4 \left\{ (\pi(1-2\dot{r}_h) + 2\Lambda) \right\} \right. \\ &\quad \left. - 3 \left\{ r_h^2(1-2\dot{r}_h - \Lambda r_h^2) - Q^2 \right\} \right. \\ &\quad \left. \times \ln \left(\frac{4\sqrt{\pi}(1-2\dot{r}_h)}{(1-2\dot{r}_h - \Lambda r_h^2) - Q^2 r_h^{-2}} \right) \right].\end{aligned}\quad (71)$$

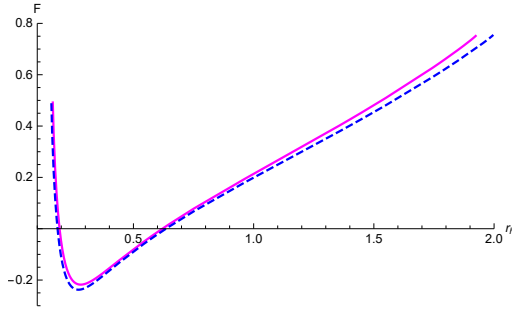


Figure 10. Plot of Helmholtz free energy in the absence of LIV theory and Helmholtz free energy under LIV theory for $Q = 0.1$, $\lambda = 1$, $\Lambda = 0.1$, $m = 0.1$ and $r_h = 0.3$.

In Fig. 10, we plot Helmholtz free energy both with and without the influence of LIV theory. Both the Helmholtz free energy show a similar pattern, at first they decrease monotonically upto minimum energy level and later increase with increasing the size of black hole. The LIV theory increases the Helmholtz free energy. In comparison to smaller black holes, larger black holes are more affected by the LIV theory.

4.2. Internal energy

The internal energy of VBdS black hole is given by [88]

$$E = F + T \tilde{S}. \quad (72)$$

Using Eqs. (21), (67) and (70), the internal energy under LIV theory is calculated as

$$E = \frac{1}{6\pi r_h^3(1-2\dot{r}_h)} \left[Q^2(1+3\pi r_h^2)(1+\lambda m) + r_h^4 \left[3\pi \left((1+\lambda m) - \dot{r}_h(1+2\lambda m) \right) + (3-\pi r_h^2)(1+\lambda m)\Lambda \right] \right]. \quad (73)$$

The internal energy without LIV theory is obtain as

$$E_0 = \frac{1}{6\pi r_h^3(1-2\dot{r}_h)} \left[Q^2(1+3\pi r_h^2) + r_h^4 \left[3\pi(1-\dot{r}_h) + (3-\pi r_h^2)\Lambda \right] \right]. \quad (74)$$

We plot Fig. 11 for internal energy of VBdS black hole with and without the influence of LIV theory. For small black holes, both the internal energy are positive and show a fluctuation behaviour. However the internal energy becomes negative for large black hole implying the stability of the large black hole. One can see that there exists an event horizon radius $r_h = r_h^*$ below which the internal energy under LIV theory is greater than the internal energy without LIV theory and vice versa for $r_h > r_h^*$. The value of r_h^* is found to be 2.00781.

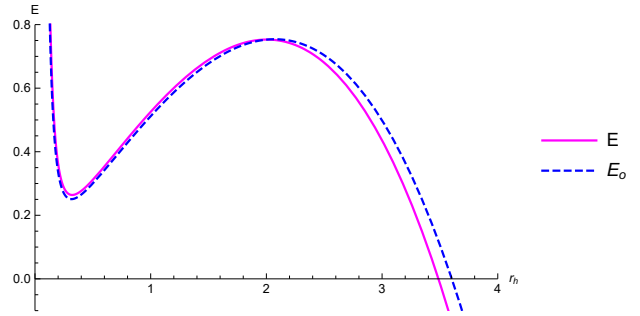


Figure 11. Internal energy of VBdS black hole with and without the influence of LIV theory for $Q = 0.1$, $\lambda = 1$, $\Lambda = 0.1$, $m = 0.1$ and $r_h = 0.3$.

4.3. Enthalpy

The enthalpy H of the black hole is given by [87]

$$H = E + P V. \quad (75)$$

First we derive the pressure from Helmholtz free energy as

$$P = -\frac{dF}{dV} = \frac{1}{16\pi^2 r_h^6(1-2\dot{r}_h)} \left[r_h^2 \left(\Sigma + \Lambda r_h^2(1+\lambda m) - 3Q^2(1+\lambda m) \right) \times \left[\pi r_h^2 + \ln \left(\frac{4\sqrt{\pi}(1-2\dot{r}_h)}{(\Sigma - \Lambda r_h^2(1+\lambda m) - Q^2(1+\lambda m)r_h^{-2})} \right) \right] \right]. \quad (76)$$

Using the Eqs. (73) and (76), we calculate the enthalpy of VBdS black hole under LIV theory as

$$H = \frac{1}{12\pi r_h^3(1-2\dot{r}_h)} \left[Q^2(2+9\pi r_h^2)(1+\lambda m) + r^4 \left[7\pi \Sigma + (6-\pi r_h^2)(1+\lambda m)\Lambda \right] + \left[r^2 \left\{ \Sigma + (1+\lambda m)\Lambda r^2 \right\} - 3Q^2(1+\lambda m) \right] \times \ln \left[\frac{4\sqrt{\pi}(1-2\dot{r}_h)}{\Sigma - \Lambda r_h^2(1+\lambda m) - Q^2(1+\lambda m)r_h^{-2}} \right] \right]. \quad (77)$$

The enthalpy of VBdS black hole in the absence of LIV theory is given by

$$H_0 = \frac{1}{12\pi r_h^3(1-2\dot{r}_h)} \left[Q^2(2+9\pi r_h^2) + r^4 \left[7\pi(1-2\dot{r}_h) + \Lambda(6-\pi r_h^2) \right] + \left[r^2(1-2\dot{r}_h + \Lambda r^2) - 3Q^2 \right] \times \ln \left[\frac{4\sqrt{\pi}(1-2\dot{r}_h)}{1-2\dot{r}_h - \Lambda r_h^2 - Q^2 r_h^{-2}} \right] \right]. \quad (78)$$

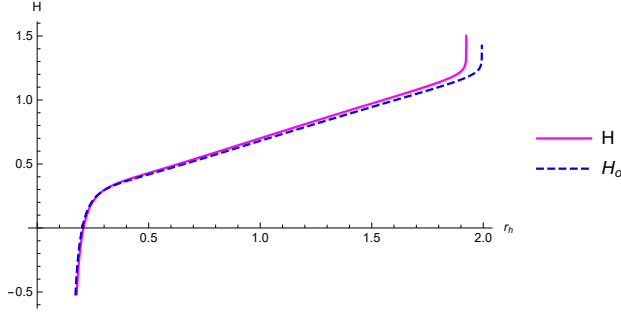


Figure 12. Enthalpy of VBdS black hole with and without LIV theory for $Q = 0.1$, $\lambda = 1$, $\Lambda = 0.1$, $m = 0.1$ and $r_h = 0.3$.

In Fig. 12, the enthalpy of VBdS black hole with and without the influence of LIV theory are plotted and illustrated the effect cause by LIV theory. We observe that LIV theory doesn't affect the small black hole but for large black hole LIV theory increases the enthalpy of the black hole.

5. Stability of Black hole

In this section we discuss the global and local stability of the black hole. The global stability of the black hole will be analyzed by using the Gibbs free energy. The local stability will also be discussed by evaluating the heat capacity and Hessian matrix.

5.1. Gibbs free energy

When the cosmological constant is interpreted as thermodynamic pressure, a new term VdP arises in the first law of black hole thermodynamics. As a consequence, the mass of the black hole is considered as the enthalpy rather than the internal energy [89–91]. Thus the first law of non-rotating charged black hole thermodynamics becomes

$$dM = T dS + V dP + \Phi dQ, \quad (79)$$

where $\Phi = \frac{Q}{r_h}$ is the electric potential. Thus, in canonical ensemble, the Gibbs free energy of the black hole in extended phase space is given by

$$G = M - TS. \quad (80)$$

The modified Gibbs free energy under LIV theory is obtained by substituting Eqs. (5), (21) and (67) in Eq. (80) as

$$G = \frac{1}{4\pi r_h^3(1-2\dot{r}_h)} \left[2\pi r_h^2(1-2\dot{r}_h) \left(r_h^2 + Q^2 - 2r_h^2\dot{r}_h - \frac{\Lambda}{3}r_h^4 \right) - \left\{ \Sigma r_h^2 - (1+\lambda m)(Q^2 + \Lambda r_h^4) \right\} \left(\pi r_h^2 + \ln \left[\frac{4\sqrt{\pi}r_h^2(1-2\dot{r}_h)}{\Sigma r_h^2 - (1+\lambda m)(Q^2 + \Lambda r_h^4)} \right] \right) \right]. \quad (81)$$

The Gibbs free energy in the absence of LIV theory is obtain as

$$G_0 = \frac{1}{4\pi r_h^3(1-2\dot{r}_h)} \left[2\pi r_h^2(1-2\dot{r}_h) \left(r_h^2 - Q^2 - 2r_h^2\dot{r}_h - \frac{\Lambda}{3}r_h^4 \right) - \left(r_h^2 - 2r_h^2\dot{r}_h - Q^2 - \Lambda r_h^4 \right) \left(\pi r_h^2 + \ln \left[\frac{4\sqrt{\pi}r_h^2(1-2\dot{r}_h)}{r_h^2 - 2r_h^2\dot{r}_h - Q^2 - \Lambda r_h^4} \right] \right) \right]. \quad (82)$$

The study of Gibbs free energy of black hole provides

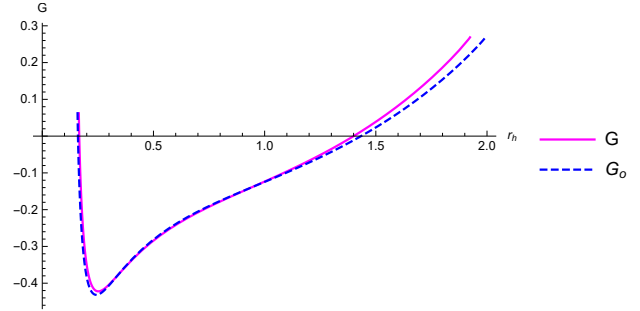


Figure 13. Gibbs free energy of VBdS black hole with or without influence of LIV theory for $Q = 0.1$, $\lambda = 1$, $\Lambda = 0.1$, $m = 0.1$ and $r_h = 0.3$.

a vital information about the global stability of black hole. The preferred phase of the system is the one that minimizes the Gibbs free energy. Gibbs free energy under LIV modification and in the absence of LIV modification are plotted in Fig. 13. Both the Gibbs free energy decrease for small black hole and increase with increasing r_h . The small black hole has lower Gibbs free energy and hence it is globally stable. The large black holes have a higher Gibbs free energy signifying a globally unstable state. Further, the black holes are more unstable under the influence of LIV theory.

5.2. Heat Capacity

The study of the heat capacity of black hole provides a vital information about its phase transitions and thermodynamic local stability. The phase transition point is the point where the heat capacity either

vanishes or diverges. The points where heat capacity vanishes are the first-type phase transition whereas the points at which the heat capacity diverges correspond to the second-type phase transition. Moreover, a stable black hole has a positive heat capacity, whereas an unstable black hole has a negative heat capacity.

The heat capacity in the absence of LIV theory is calculated using Eqs. (22) and (68) as

$$C_0 = T_h \frac{\partial S_c}{\partial T_h} = - \frac{2 \left[Q^2(1 + \pi r_h^2) - r_h^4 \{ \Lambda + \pi(1 - 2\dot{r}_h - r_h^2 \Lambda) \} \right]}{r_h^2(1 - 2\dot{r}_h + r_h^2 \Lambda) - 3Q^2}. \quad (83)$$

Substituting Eqs. (21) and (67) in Eq. (83), we find the modified heat capacity under the influence of LIV theory as

$$C = T \frac{\partial S}{\partial T} = \frac{2}{r_h^2 \left(\Sigma + \Lambda r_h^2(1 + \lambda m) \right) - 3Q^2(1 + \lambda m)} \left[Q^2(1 + \lambda m)(1 + \pi r_h^2) - \left\{ \Lambda(1 + \lambda m) + \pi \left(\Sigma - \Lambda r_h^2(1 + \lambda m) \right) \right\} \right]. \quad (84)$$

In order to study the influence of LIV theory on the

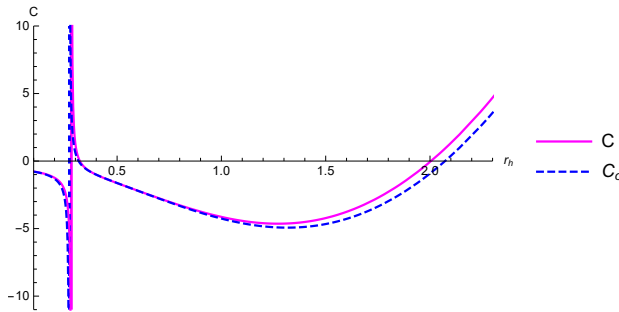


Figure 14. Heat capacity of VBdS black hole with and without LIV theory with respect to radius of event horizon r_h for $Q = 0.1$, $\lambda = 1$, $\Lambda = 0.1$, $m = 0.1$ and $\dot{r}_h = 0.3$.

phase transition and stability of the black hole, we plot C_0 and C in Fig. 14. For the heat capacity in the absence of LIV theory, the second-type phase transition point is $r_h = 0.271375$ and the first-type phase transition points are $r_h = 0.315466$ and $r_h = 2.07203$ for the above set of parameters. However due to LIV theory, the second-type phase transition point is $r_h = 0.280751$ and the first-type phase transition points are $r_h = 0.321609$ and $r_h = 2.00468$. We

conclude that the positions of phase transitions are affected by LIV theory. It is worth mentioning that the both the heat capacities are positive for large horizon radius implying the stability for large black holes. The stable and unstable range of the heat capacities are displayed in Table 4.

5.3. Hessian matrix

Another approach to check the local stability of black holes is by using Hessian matrix of the Helmholtz free energy. This matrix involve the second order derivatives of Helmholtz free energy with respect to Hawking temperature and chemical potential ($\phi = \frac{\partial M}{\partial Q}$). The Hessian matrix is defined as

$$\tilde{\mathcal{H}} = \begin{pmatrix} \tilde{\mathcal{H}}_{aa} & \tilde{\mathcal{H}}_{ab} \\ \tilde{\mathcal{H}}_{ba} & \tilde{\mathcal{H}}_{bb} \end{pmatrix} \quad a, b = 1, 2, \quad (85)$$

where $\tilde{\mathcal{H}}_{11} = \frac{\partial^2 F}{\partial T^2}$, $\tilde{\mathcal{H}}_{12} = \frac{\partial^2 F}{\partial T \partial \phi}$, $\tilde{\mathcal{H}}_{21} = \frac{\partial^2 F}{\partial \phi \partial T}$ and $\tilde{\mathcal{H}}_{22} = \frac{\partial^2 F}{\partial \phi^2}$. The determinant of the Hessian matrix is found to be zero. So, one of the eigenvalue of the matrix (85) is zero. The other eigenvalue is given by the trace of the matrix. The trace of the Hessian matrix must be positive for the black hole to be locally stable. The trace of the Hessian matrix is calculated as

$$\tau = T_r(\tilde{\mathcal{H}}) = \tilde{\mathcal{H}}_{11} + \tilde{\mathcal{H}}_{22}, \quad (86)$$

where

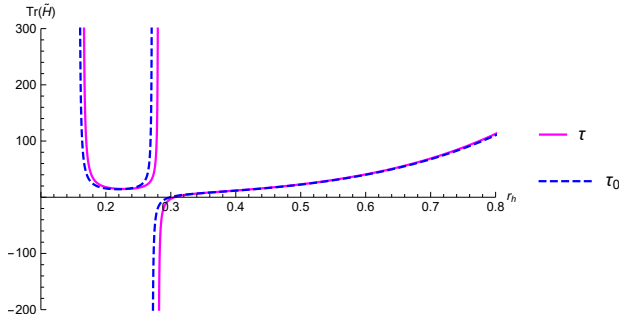
$$\begin{aligned} H_{11} &= 8\pi r_h^3 (1 - 2\dot{r}_h) \frac{\Sigma_1}{\Sigma_2}, \\ H_{22} &= \frac{1}{4\pi Q^2 (1 - 2\dot{r}_h)} \left[2(1 + \lambda m)(3Q^2 + \Lambda r^4) \right. \\ &\quad + \frac{\Theta}{r_h^2 \left(\Sigma - \Lambda r^2(1 + \lambda m) \right) - Q^2(1 + \lambda m)} \\ &\quad \left. \times \ln \left\{ \frac{4\sqrt{\pi}(1 - 2\dot{r}_h)}{(\Sigma - \Lambda r_h^2(1 + \lambda m)) - Q^2(1 + \lambda m)r_h^{-2}} \right\} \right] \end{aligned} \quad (87)$$

and the notations Σ_1 , Σ_2 and Θ are defined as

Table 4. Stable and unstable range of Vaidya-Bonner-de Sitter black hole with and without LIV theory.

	Stable range	Unstable range
Heat capacity without LIV theory (C_0)	$0.271375 < r_h < 0.3$	$0 < r_h < 0.271375$
Heat capacity under LIV theory (C)	$0.280751 < r_h < 0.321609$	$0 < r_h < 0.280751$
	$2.00468 < r_h$	$0.321609 < r_h < 2.00468$

$$\begin{aligned}
\Sigma_1 &= Q^2(1 + \lambda m)(1 + \pi r_h^2) + r_h^4 [\Lambda(1 + \lambda m)(\pi r_h^2 - 1) \\
&\quad - \Sigma \pi], \\
\Sigma_2 &= [3Q^2(1 + \lambda m) - (\Sigma + (1 + \lambda m)\Lambda r_h^2)r_h^2] \\
&\quad \times [r_h^2(\Sigma - \Lambda r_h^2(1 + \lambda m)) - Q^2(1 + \lambda m)], \\
\Theta &= 2[3Q^4(1 + \lambda m)^2 - Q^2 r_h^2(1 + \lambda m)\{(1 + \pi r_h^2)\Sigma \\
&\quad + 2\Lambda r_h^2(2 + \pi r_h^2)(1 + \lambda m)\} + r_h^6\{\Sigma \Lambda(1 + \lambda m) \\
&\quad (1 + \pi r_h^2) + \pi \Sigma^2 + r_h^2 \Lambda^2(1 + \lambda m)^2(1 - 2\pi r_h^2)\}]. \tag{88}
\end{aligned}$$

**Figure 15.** Trace of Hessian matrix with and without the influence of LIV theory for $Q = 0.1$, $\lambda = 1$, $\Lambda = 0.1$, $m = 0.1$ and $r_h = 0.3$.

We plot the trace of the Hessian matrix with respect to event horizon radius in Fig. 15. In the absence of LIV theory, the black holes in the ranges $0.158613 < r_h < 0.271375$ and $0.299026 < r_h < \infty$ are stable while under the influence of LIV theory the stable ranges are found to be $0.164393 < r_h < 0.280751$ and $0.305731 < r_h < \infty$. The LIV theory affects the stability range of the black hole. Moreover, it is worth mentioning that the large black holes are locally stable.

6. Conclusion

In this paper, the quantum tunneling radiation of fermions near the event horizon of VBdS black hole is investigated by using the Rarita-Schwinger-Hamilton-Jacobi equation under the influence of

LIV modification. Based on LIV modification, the corrected tunneling rate and the Hawking temperature are derived and found to be dependent on the LIV parameter and mass of the particle. If we take $\lambda = 0$, the results are consistent with the paper [69]. The thermal fluctuations of VBdS black hole under the influence of LIV modification is also investigated. We use first-order logarithmic corrections to calculate the corrected entropy of VBdS black hole under LIV modification. Further, the modification due to LIV modification in the thermodynamic quantities such as Helmholtz free energy, internal energy, enthalpy, Gibbs free energy, and heat capacity are studied. The results of the paper show that under the influence of LIV modification the above thermodynamic quantities tend to increase. In our graphical analysis, it is observed that the LIV modification affects the thermodynamic quantities of large black holes but it does not affect the small black hole. The stability of black hole is investigated by using the Gibbs free energy, heat capacity, and Hessian matrix. The local stability range of VBdS black hole under LIV modification is displayed in Table 4. From the above analysis, it is observed that large black holes are locally stable.

Further, the thermodynamic behaviour of VBdS black hole in extended phase space is discussed. By treating the cosmological constant as a thermodynamic pressure, we derive the equation of state under LIV modification. Similar to Van der Waals liquid-gas system in the isotherms of the VBdS black holes, we observe a region where the condition of stable equilibrium violates. The unphysical oscillating part in the isotherm should be replaced by an isobar, which represents the liquid-gas coexistence line. For different conjugate variables $P - \tilde{v}$, $P - V$ and $T - S$, we investigate the phase transitions and positions of the boundary of two phase coexistence line using Maxwell's equal-area law and also study the influence of LIV modification on the phase transition points. In the $P - \tilde{v}$ and $P - V$ planes, the length of the isobar decreases with increasing the temperature. Further, it is noted that the LIV modification increases the length of phase transition process and the transition of liquid phase to gas phase occurs at a lower pressure due to LIV modification. Similarly in $T - S$ diagram, we observe that increasing the pressure tends to decrease the length of isobar. It is noted that the liquid-gas

coexistence region in $T - S$ diagram increases and phase transition occurs at lower temperature under LIV modification.

Acknowledgements

The authors also acknowledge the anonymous reviewers for valuable suggestions and comments to improve the paper.

Declaration of competing interest

The authors declare that they have no known competing financial interests or personal relationships that could have appeared to influence the work reported in this paper

References

- [1] B. P. Abbott, et al., Phys. Rev. Lett. **116**, 061102 (2016)
- [2] B. P. Abbott, et al., Phys. Rev. X **9**, 031040 (2019)
- [3] K. Akiyama, et al., Astrophys. J. Lett. **875**, (2019) L1.
- [4] K. Akiyama, et al., Astrophys. J. Lett. **875**, L2 (2019)
- [5] K. Akiyama, et al., Astrophys. J. Lett. **875**, L3 (2019)
- [6] S. W. Hawking, Nature **248**, 30 (1974)
- [7] S. W. Hawking, Commun. Math. Phys. **43**, 199 (1975)
- [8] G. W. Gibbons, and S. W. Hawking, Phys. Rev. D **15**, 2752 (1977)
- [9] T. Damour, and R. Ruffini, Phys. Rev. D **14**, 332 (1976)
- [10] C. W. Robson, L. D. M. Villari, and F. Biancalana, Phys. Rev. D **99**, 044042 (2019)
- [11] A. Ovgun, and I. Sakalli, Annals Phys. **413**, 168071 (2020)
- [12] P. Kraus, and F. Wilczek, Nucl. Phys. B **433**, 403 (1995)
- [13] P. Kraus, and F. Wilczek, Nucl. Phys. B **437**, 231 (1995)
- [14] M. K. Parikh, and F. Wilczek, Phys. Rev. Lett. **85**, 5042 (2000)
- [15] M. K. Parikh, Int. J. Mod. Phys. D **13**, 2351 (2004)
- [16] M. Angheben, M. Nadalini, L. Vanzo, and S. Zerbini, J. High Energy Phys. **05**, 014 (2005)
- [17] K. Srinivasan, and T. Padmanabhan, Phys. Rev. D **60**, 024007 (1999)
- [18] S. Shankaranarayanan, K. Srinivasan, and T. Padmanabhan, Mod. Phys. Lett. A **16**, 571 (2001)
- [19] S. Shankaranarayanan, T. Padmanabhan, and K. Srinivasan, Class. Quantum Grav. **19**, 2671 (2002)
- [20] J. Y. Zhang, and Z. Zhao, Nucl. Phys. B **725**, 173 (2005)
- [21] J. Y. Zhang, and Z. Zhao, Phys. Lett. B **638**, 110 (2006)
- [22] R. Kerner, and R. B. Mann, Phys. Lett. B **665**, 277 (2008)
- [23] R. Kerner, and R. B. Mann, Class. Quantum Grav. **25**, 095014 (2008)
- [24] M. A. Rahman, and M. I. Hossain, Phys. Lett. B **712**, 1 (2012)
- [25] T. I. Singh, I. A. Meitei, and K. Y. Singh, Astrophys. Space Sci. **345**, 177 (2013)
- [26] R. Banerjee, and B. R. Majhi, J. High Energy Phys. **06**, 095 (2008)
- [27] R. Banerjee, and B. R. Majhi, Phys. Lett. B **662**, 62 (2008)
- [28] R. J. Adler, P. Chen, and D. I. Santiago, Gen. Rel. Grav. **33**, 2101 (2001)
- [29] D. Y. Chen, H. Wu, and H. Yang, Adv. High Energy Phys. **2013**, 432412 (2013)
- [30] D. Y. Chen, Q. Q. Jiang, P. Wang, and H. Yang, J. High Energy Phys. **2013**, 176 (2013)
- [31] X. Q. Li, Phys. Lett. B **763**, 80 (2016)
- [32] A. Ovgun, and K. Jusufi, Eur. Phys. J. Plus **131**, 177 (2016)
- [33] Z. W. Feng, H. L. Li, X. T. Zu, and S. Z. Yang, Eur. Phys. J. C **76**, 212 (2016)
- [34] E. C. Vagenas, S. M. Alsaleh, and A. F. Ali, EPL **120**, 40001 (2017)
- [35] T. I. Singh, Y. K. Meitei, and I. A. Meitei, Int. J. Mod. Phys. A **35**, 2050018 (2020)
- [36] B. Carr, H. Mentzer, J. Mureika, and P. Nicolini, Eur. Phys. J. C **80**, 1166 (2020)
- [37] Y. P. Singh, and T. I. Singh, J. High Energy Phys. **2023**, 54 (2023)
- [38] G. Lambiase, and F. Scardigli, Phys. Rev. D **97**, 075003 (2018)
- [39] M. A. Anacleto, F. A. Brito, C. V. Garcia, et al.: Phys. Rev. D **100**, 105005 (2019)
- [40] S. K. Jha, and A. Rahaman, Eur. Phys. J. C **82**, 411 (2022)
- [41] J. Magueijo, and L. Smolin, Phys. Rev. Lett. **88**, 190403 (2002)
- [42] G. Amelino-Camelia, New J. Phys. **6**, 188 (2004)
- [43] S. I. Kruglov, Phys. Lett. B **718**, 228 (2012)
- [44] S. Chen, J. Jing, and H. Liao, Phys. Lett. B **751**, 474 (2015)
- [45] J. Zhang, M. Liu, Z. Liu, et al., Gen. Relativ. Gravit. **52**, 105 (2020)
- [46] B. Sha, and Z. E. Liu, Eur. Phys. J. C **82**, 648 (2022)
- [47] R. Li, Q. T. Ding, and S. Z. Yang, EPL **138**, 60001 (2022)
- [48] J. Zhang, Z. Liu, B. Sha, X. Tan, Y. Liu, and S. Yang, Adv. High Energy Phys. **2020**, 2742091 (2020)
- [49] P. Jin, Y. S. Zheng, and L. Kai, Acta Phys. Sin. **68**, 190401 (2019)
- [50] B. Sha, Z. E. Liu, Y. Z. Liu, et al., Chinese Phys. C **44**, 125104 (2020)
- [51] S. Z. Yang, K. Lin, J. Li, and Q. Q. Jiang, Adv. High Energy Phys. **2016**, 7058764 (2016)
- [52] Z. E. Liu, J. Zhang, and S. Z. Yang, Results Phys. **29**, 104710 (2021)
- [53] Z. E. Liu, J. Zhang, and S. Z. Yang, Front. Phys. **9**, 762279 (2021)
- [54] Y. P. Singh, T. I. Singh, I. A. Meitei, and A. K. Singh, Int. J. Mod. Phys. D **31**, 2250106 (2022)
- [55] Y. O. Laxmi, T. I. Singh, and I. A. Meitei, Gen. Relativ. Gravit. **54**, 77 (2022)
- [56] N. Media, Y. O. Laxmi, T. I. Singh, Int. J. Geom. Meth. Mod. Phys. **20**, 2350217 (2023)
- [57] S. W. Hawking, and D. N. Page, Comm. Math. Phys. **87**, 577 (1983)
- [58] A. Chamblin, R. Emparan, C. V. Johnson, and R. C. Myers, Phys. Rev. D **60**, 104026 (1999)
- [59] B. P. Dolan, Class. Quantum Grav. **28**, 125020 (2011)
- [60] D. Kubiznak, and R. B. Mann, J. High Energy Phys. **2012**, 33 (2012)
- [61] D. Kubiznak, R. B. Mann, and M. Teo, Class. Quantum Grav. **34**, 063001 (2017)
- [62] R. G. Cai, L. M. Cao, L. Li, and R. Q. Yang, J. High Energy Phys. **2013**, 5 (2013)
- [63] R. Zhao, H. H. Zhao, M. S. Ma, and L. C. Zhang, Eur. Phys. J. C **73**, 2645 (2013)
- [64] B. P. Dolan, D. Kastor, D. Kubiznak, et al., Phys. Rev. D **87**, 104017 (2013)
- [65] B. R. Majhi, and S. Samanta, Phys. Lett. B **773**, 203 (2017)
- [66] D. C. Zou, S. J. Zhang, and B. Wang, Phys. Rev. D **89**, 044002 (2014)
- [67] K. Jafarzade, J. Sadeghi, B. E. Panah, and S. H. Hendi, Ann. Phys. **432**, 168577 (2021)
- [68] A. Kumar, A. Sood, J. K. Singh, A. Beesham, and S. G. Ghosh, Phys. Dark Universe **40**, (2023) 101220.
- [69] R. Li, and J. Wang, Phys. Lett. B **813**, 136035 (2021)
- [70] A. Chamblin, R. Emparan, C. V. Johnson, et al., Phys. Rev. D **60**, 064018 (1999)
- [71] J. X. Zhao, M. S. Ma, L. C. Zhang, H. H. Zhao, and R. Zhao, Astrophys. & Space Sci. **352**, 763 (2014)
- [72] A. Belhaj1, M. Chabab, H. El moumni, K. Masmar, and

- M. B. Sedra, Eur. Phys. J. C **75**, 71 (2015)
- [73] H. F. Li, X. Y. Guo, H. H. Zhao, and R. Zhao, Gen. Relativ. Gravit. **49**, 111 (2017)
- [74] E. Spallucci, and A. Smailagic, Phys. Lett. B **723**, 436 (2013)
- [75] E. Spallucci, and A. Smailagic, J. Grav. **2013**, 525696 (2013)
- [76] L. C. Zhang, H. H. Zhao, R. Zhao, and M. S. Ma, Adv. High Energy Phys **2014**, 816728 (2014)
- [77] X. Y. Guo, H. F. Li, and R. Zhao, Eur. Phys. J. Plus **134**, 277 (2019)
- [78] M. Sharif, and Q. A. T. Mughani, Eur. Phys. J. Plus **136**, 284 (2021)
- [79] W. B. Bonner, and P. C. Vaidya, Gen. Relativ. Gravit. **1**, 127 (1970)
- [80] J. Ellis, N. E. Mavromatos, and D. V. Nanopoulos, Phys. Lett. B **293**, 37 (1992)
- [81] S. I. Kruglov, Mod. Phys. Lett. A **28**, 1350014 (2013)
- [82] T. Jacobson, S. Liberati, D. Mattingly, and A. Erratum, Nature **424**, 1019 (2003)
- [83] F. Simovic, R. B. Mann, Class. Quantum Grav. **36**, 014002 (2019)
- [84] Y. Ma, Y. Zhang, L. Zhang, et al., Eur. Phys. J. C **81**, 42 (2021)
- [85] P. Pradhan, Universe **5**, (2) (2019) 57.
- [86] S. Das, P. Majumdar, and R. K. Bhaduri, Class. Quantum Grav. **19**, 2355 (2002)
- [87] Z. Akhtar, R. Babar, and R. Ali, Ann. Phys. **448**, 169190 (2023)
- [88] B. Pourhassan, and S. Upadhyay, Eur. Phys. J. Plus **136**, 311 (2021)
- [89] C. Ding, C. Liu, A. Wang and J. Jing, Phys. Rev. D **94**, 124034 (2016)
- [90] D. Kastor, S. Ray and J. Traschen, Class. Quantum Grav. **26**, 195011 (2009)
- [91] C. Ding, Y. Shi, J. Chen, Y. Zhou, C. Liu, Chin. Phys. C **47**, 045102 (2023)